AFRL-ML-TY-TP-2001-4502

A CONSTITUTIVE STUDY OF TWO-PHASE MATERIALS PART II. MAXWELL BINDER (POSTPRINT)

Han Zhu and Shalu Batra
Civil and Environmental Engineering Department
Arizona State University
Tempe, AZ 862-87-5306

Jeff W. Rish, III
NSWCDD Coastal Systems Station, Code R23
6703 West Highway 98
Panama City, FL 32407-7001

July 2001

AIR FORCE RESEARCH LABORATORY
MATERIALS AND MANUFACTURING DIRECTORATE

■ **Air Force Materiel Command** ■ **United States Air Force** ■ **Tyndall Air Force Base, FL 32403-5323**

REPORT DOCUMENTATION PAGE	Form Approved OMB No. 0704-0188

1. REPORT DATE *(DD-MM-YYYY)*	2. REPORT TYPE	3. DATES COVERED *(From - To)*
1 JUL 2001	Journal Article - POSTPRINT	

4. TITLE AND SUBTITLE	
A Constitutive Study of Two-phase Materials Part II. Maxwell Binder (POSTPRINT)	5a. CONTRACT NUMBER
	5b. GRANT NUMBER
	5c. PROGRAM ELEMENT NUMBER
6. AUTHOR(S) Han Zhu*, Jeff W. Rish, III%, and Shalu Batra*	5d. PROJECT NUMBER
	5e. TASK NUMBER
	5f. WORK UNIT NUMBER

7. PERFORMING ORGANIZATION NAME(S) AND ADDRESS(ES)	8. PERFORMING ORGANIZATION REPORT NUMBER
*Civil and Environmental Engineering Department; Arizona State University; Tempe, AZ 86287-5306 %NSWCDD Coastal Systems Station, Code R23; 6703 West Highway 98; Panama City, FL 32407-7001	

9. SPONSORING/MONITORING AGENCY NAME(S) AND ADDRESS(ES)	10. SPONSOR/MONITOR'S ACRONYM(S)
Air Force Research Laboratory Materials and Manufacturing Directorate Airbase Technologies Division 139 Barnes Drive, Suite 2 Tyndall Air Force Base, FL 32403-5323	AFRL/MLQ 11. SPONSOR/MONITOR'S REPORT NUMBER(S) AFRL-ML-TY-TP-2001-4502

12. DISTRIBUTION/AVAILABILITY STATEMENT
DISTRIBUTION A. Approved for public release; distribution unlimited.
Available only to DTIC users. U.S. Government or Federal Purpose Rights License.

13. SUPPLEMENTARY NOTES
Distribution Code 20: JOURNAL ARTICLES; DTIC USERS ONLY. Published in Computers and Geotechnics, Volume 28, Issue 5, July 2001, Pages 309-323

14. ABSTRACT

This article presents a constitutive study of a two-phase composite based on the authors' previous paper [Zhu H, Rish III JW, Dass WC. Constitutive relation for two-phase particular materials. I: elastic binder. Computers and Geotechnics 1997;20(3):303–23] with inclusions/particles in the composite behaving elastically, but the binder/matrix being visco-elastic of Maxwell type. The basic-cell technique and binder-contact laws are employed in deriving the stress–strain equations in the integral representation. It is shown that the overall stress–strain response of this two-phase composite can be described by an equivalent multi-axial visco-elastic model of four-Maxwell-elements in parallel. The application of this study is aimed at providing a mechanics/physics based justification for employing the multi-Maxwell-elements model in characterizing asphalt concrete and other related issues.

15. SUBJECT TERMS
composite, matrix/binder, inclusion/particles, visco-elastic, maxwell element, asphalt concrete

16. SECURITY CLASSIFICATION OF: a. REPORT	b. ABSTRACT	c. THIS PAGE	17. LIMITATION OF ABSTRACT	18. NUMBER OF PAGES	19a. NAME OF RESPONSIBLE PERSON
U	U	U	UU	15	AFRL/MLQ 19b. TELEPHONE NUMBER *(Include area code)* 850 283 6002

Reset **Standard Form 298** (Rev. 8/98)
Prescribed by ANSI Std. Z39.18

ELSEVIER

Computers and Geotechnics 28 (2001) 309–323

COMPUTERS AND GEOTECHNICS

www.elsevier.com/locate/compgeo

A constitutive study of two-phase materials Part II. Maxwell binder

Han Zhu [a,*], Jeff W. Rish III [b], Shalu Batra [a]

[a]*Civil and Environmental Engineering Department, Arizona State University, Tempe, AZ 86287-5306, USA*
[b]*NSWCDD Coastal Systems Station, Code R23, 6703 West Highway 98, Panama City, FL 32407-7001, USA*

Received 17 August 2000; received in revised form 6 December 2000; accepted 29 December 2000

Abstract

This article presents a constitutive study of a two-phase composite based on the authors' previous paper [Zhu H, Rish III JW, Dass WC. Constitutive relation for two-phase particular materials. I: elastic binder. Computers and Geotechnics 1997;20(3):303–23] with inclusions/particles in the composite behaving elastically, but the binder/matrix being visco-elastic of Maxwell type. The basic-cell technique and binder-contact laws are employed in deriving the stress–strain equations in the integral representation. It is shown that the overall stress–strain response of this two-phase composite can be described by an equivalent multi-axial visco-elastic model of four-Maxwell-elements in parallel. The application of this study is aimed at providing a mechanics/physics based justification for employing the multi-Maxwell-elements model in characterizing asphalt concrete and other related issues. © 2001 Elsevier Science Ltd. All rights reserved.

Keywords: Composite; Matrix/binder; Inclusion/particles; Visco-elastic; Maxwell element; Asphalt concrete

1. Introduction

Compared with the rigidness of matrixes or binders, particles or inclusions in many two-phase engineering composites are much stiffer. So, assuming particles or inclusions to be elastic is a reasonable simplification in conducting the constitutive analysis of the composite. On the other hand, most matrixes or binders are viscous

* Corresponding author: Fax: +1-480-9650557.
E-mail address: han.zhu@asu.edu (H. Zhu).

0266-352X/01/$ - see front matter
PII: S0266-352X(01)00003-9

in nature. Now the question is, when blending the two (matrix/binder and particles/inclusions) together, what is the overall constitutive behavior of the composite?

There are many studies done in response to answering this question in different technical areas. Schapery [3] and Hashin [4] published quite a few well-known articles in the subject of visco-elastic behaviors of composite materials. Certain sands exhibit creep characteristics. Murayama [5] proposed a theoretical model to describe it. Kuhn [6] selected his PhD theme on the study of sand creep. Meegoda and Chang [7] attempted to incorporate the visco-elastic binder effect into DEM calculations in simulation of asphalt concrete. Experimental studies of this subject have also made important progress, which include the work of Lacerda [8] and Murayama et. al. [9], etc. Zhu and Nodes [10] presented a fabric-tensors based approach in analyzing the angularity effect of aggregate in asphalt concrete.

In the authors' previous article [1] (referred hereinafter as part I), a micro-mechanical analysis to a two-phase composite with elastic binder/matrix and elastic particles/inclusions has been carried out. This article extends the work done in part I in the context that now the binder is taken to be a Maxwell type of visco-elastic material. The objective of this study is to derive the stress–strain equations that govern the mechanical behavior of a composite with elastic inclusions/particles and a Maxwell matrix/binder. Two tools are employed to implement this study. The first one is the basic cell method, and a description of this method is given in part I. The second one is the binder-contact laws with Maxwell type of binder material, and the details about the laws can be found in [2]. There are other types of visco elastic binder/matrix materials, but the reason to select Maxwell type in this study is that there are quite a number of investigations [11,12] that are reported to employ generalized Maxwell models in simulating the mechanical behavior of asphalt concrete.

Since the most steps in the derivation needed to complete the current analysis are identical to what done in the elastic binder case, which can be found in part I, we will list only those here in which the viscous effect is presented. At the same time, we also refer to the definitions of symbols and notations given in Nomenclature in part I to both parts of this work.

2. Maxwell binder effect

Fig. 1 shows a cross-sectional view of a two-dimensional circular particle packing structure. The particles which are all of equal radius, a, are periodically spaced in a hexagonal array in a binder material with the distance between the centers of two adjacent particles being d. Two packing directions known as the closest packing direction (CPD) and the mid-closest packing direction (Mid-CPD) can then be defined. An x–y coordinate system is subsequently introduced that the x-axis and y-axis are parallel to CPD and Mid-CPD, respectively.

Based upon this packing structure, we select a basic cell (labeled A in Fig. 1 in part I), and will do the analysis upon the configuration of this basic cell (see Fig. 2).

For the elastic binder, the force-displacement or stress–strain is derived using the constitutive relation which is time-independent. When the binder becomes visco-

elastic, the constitutive relation now is time dependent. However, we attempt to convert or express such time-dependent nature of the constitutive relation with an integral representation so symbolically, the micro-mechanics derivation process will

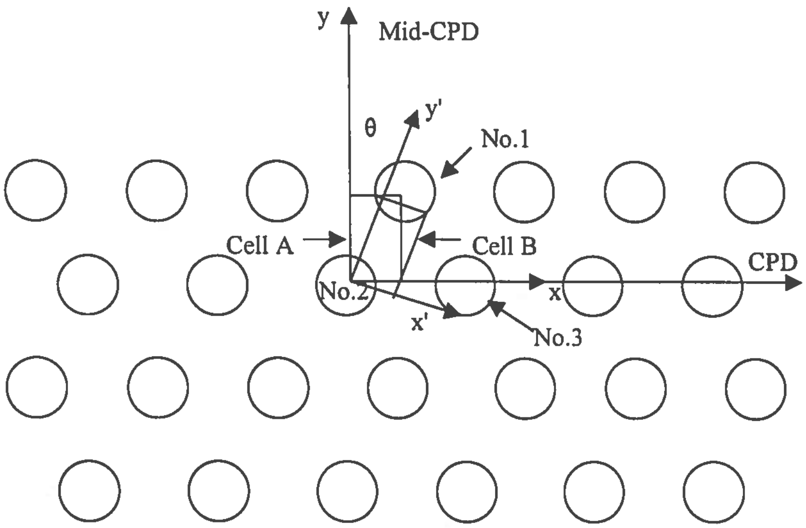

Fig. 1. Sketch of the configuration for a two phase material.

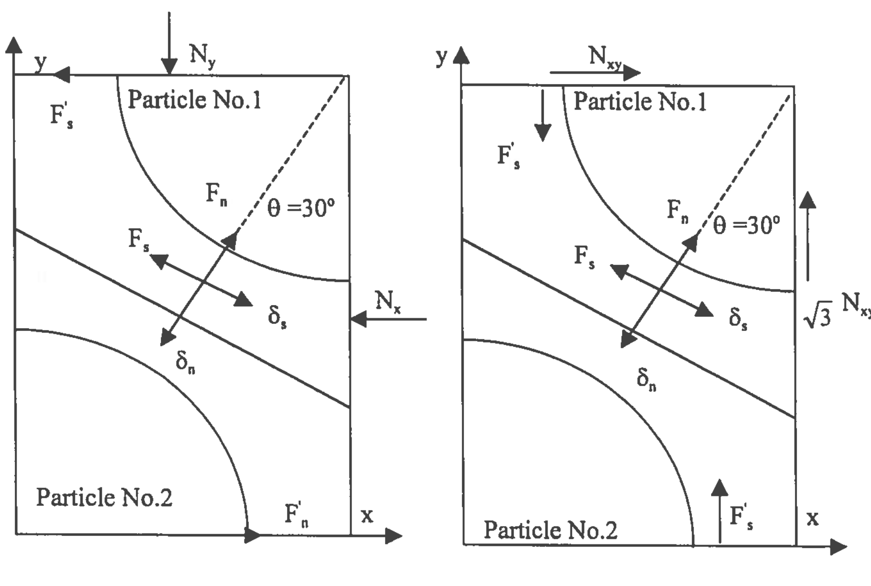

a. Normal Forces b. Shear Forces

Fig. 2. Basic cells under (a) normal forces and (b) shear forces.

be equivalent to that of the elastic binder case. The relationship of pressure–volumetric-strain for the Maxwell binder can be described by:

$$\frac{\dot{p}}{K_b} + \frac{p}{\eta_b} = \dot{\varepsilon}_b \tag{1-1}$$

where, p is the hydrostatic pressure, K_b and η_b are the binder bulk modulus and viscosity constant, respectively.

Using the similar approach given in Appendix A in part I, the averaged binder pressure $\bar{p}$ in the cell and the cell strains ε_x and ε_y obey the following equations:

$$\bar{p} = K^*(\varepsilon_x + \varepsilon_y) - < \varepsilon_x + \varepsilon_y >^* \tag{1-2}$$

where, $< >^*$ represents an integral representation as defined below:

$$< f >^* = g^* \int_0^t e^{-g^*(t-t_1)} K^* f \, dt_1 \tag{1-3}$$

and

$$g^* = \frac{V_b E^*}{\eta_b} \tag{1-4}$$

where, V_b is the binder volume fraction, E^* and K^* are the equivalent bulk and Young's modulus [1].

Another aspect of viscous effect involves the binder-contact laws. The tangential and normal binder-contact compliances for Maxwell binder can be generally expressed by:

$$\begin{aligned} K_s \delta_s &= F_s + g_s \textstyle\int_0^t F_s \, dt \\ K_n \delta_n &= F_n + g_n \textstyle\int_0^t F_n dt \end{aligned} \tag{1-5a, b}$$

where, δ_n and δ_s are the normal and tangential relative approaches, F_n and F_s are the normal and tangential contact forces, K_n and K_s are the normal and tangential coefficient of contact stiffness. g_n and g_s are defined as:

$$g_n = \frac{C_{nb} G_b}{(C_{nb} + C_{np})\eta_b}, \quad g_s = \frac{C_{sb} G_b}{(C_{sb} + C_{sp})\eta_b} \tag{1-6a, b}$$

and C_{nb}, C_{np}, C_{sb} and C_{sp} are so called the elastic binder normal contact compliance, the elastic particle normal contact compliance, the elastic binder shear contact compliance and the elastic particle shear contact compliance, respectively. Their definitions can be found in [2].

If we multiply the following function:

$$e^{\int_0^t g_s dt_1}$$

to the both sides of Eq. (1-5a), it gives rise to, after a few steps of manipulation, an equivalent expression of Eq. (1-5a):

$$F_s = K_s\delta_s - <\delta_s>^s \quad (1\text{-}7)$$

where, the definition for $< >^s$ is:

$$<f>^s = g_s\int_0^t e^{-g_s(t-t_1)}K_s f\, dt_1 \quad (1\text{-}8)$$

It appears that the term $<\delta_s>^s$ in Eq. (1-7) represents the viscous portion of the shear response for the binder-contact force-deformation interaction. Similarly, an equivalency to Eq. (1-5b) can be expressed by:

$$F_n = K_n\delta_n - <\delta_n>^n \quad (1\text{-}9)$$

where, the definition for $< \ >^n$ is:

$$<f>^n = g_n\int_0^t e^{-g_n(t-t_1)}K_n f\, dt_1 \quad (1\text{-}10)$$

3. Basic cell analysis

3.1. Normal deformation

Incorporating the Maxwell viscous effect as stated in Eqs. (1-1) to (1-9) into the derivation of the cell-level stress–strain relationships when the cell is subjected to normal forces (see the details of derivation in part I), we obtain the following two integral equations between the cell stresses (σ_x, σ_y) and the cell strains (ε_x, ε_y):

$$\sigma_x = Q_{11}\varepsilon_x + Q_{12}\varepsilon_y - \frac{5}{4\sqrt{3}} < \varepsilon_x >^n - \frac{\sqrt{3}}{4} < \varepsilon_y >^n - \frac{\sqrt{3}}{4} < \varepsilon_x - \varepsilon_y >^s - < \varepsilon_x + \varepsilon_y >^*$$
$$\sigma_y = Q_{12}\varepsilon_x + Q_{22}\varepsilon_y - \frac{\sqrt{3}}{4} < \varepsilon_x >^n - \frac{3\sqrt{3}}{4} < \varepsilon_y >^n + \frac{\sqrt{3}}{4} < \varepsilon_x - \varepsilon_y >^s - < \varepsilon_x + \varepsilon_y >^*$$
$$(2\text{-}1a, b)$$

where, Q_{11}, Q_{12} and Q_{22} are the elements in the on-axis stiffness matrix [1].

3.2. Shear deformation

As stated in part I, the cell's elastic shear stiffness consists of $Q_{66} = Q_{66}' + Q_{66}''$, where Q_{66}' and Q_{66}'' are non-contact part and contact part controlled shear stiffness, respectively [1].

Following the steps analogous to what given in Section 4 in part I, and at the same time incorporating the binder's visco-elastic effect, we can obtain the cell shear stress (σ_{xy}) — cell shear strain (ε_{xy}) governing equation:

$$\sigma_{xy} = Q_{66} 2\varepsilon_{xy} - \frac{\sqrt{3}}{4} < 2\varepsilon_{xy} >^n - \frac{3\sqrt{3}}{20} < 2\varepsilon_{xy} >^s - < 2\varepsilon_{xy} >' \tag{2-2}$$

where

$$< \varepsilon_{xy} >' = g' \int_0^t \left[e^{-g'(t-t_1)} Q'_{66} \ \varepsilon_{xy} \right] dt_1, \quad g' = \frac{Q'_{66} \ V_b}{\eta_{bs}} \tag{2-3}$$

Eqs. (2-1), (2-2) and (2-3) are derived when the cell's x and y coordinates coincide with CPD and Mid-CPD ($\theta = 0$) [1]. To put those equations in a matrix form, we have:

$$\begin{aligned}
\begin{bmatrix} \sigma_x \\ \sigma_y \\ \sigma_{xy} \end{bmatrix}_{\theta=0} &= \begin{bmatrix} Q_{11} & Q_{12} & 0 \\ Q_{12} & Q_{22} & 0 \\ 0 & 0 & Q_{66} \end{bmatrix} \begin{bmatrix} \varepsilon_x \\ \varepsilon_y \\ 2\varepsilon_{xy} \end{bmatrix}_{\theta=0} - \frac{\sqrt{3}}{4} \begin{bmatrix} 5/3 & 1 & 0 \\ 1 & 3 & 0 \\ 0 & 0 & 1 \end{bmatrix} \\
&\times \begin{bmatrix} < \varepsilon_x >^n \\ < \varepsilon_y >^n \\ < 2\varepsilon_{xy} >^n \end{bmatrix}_{\theta=0} - \frac{\sqrt{3}}{4} \begin{bmatrix} 1 & -1 & 0 \\ -1 & 1 & 0 \\ 0 & 0 & 0.6 \end{bmatrix} \\
&\times \begin{bmatrix} < \varepsilon_x >^s \\ < \varepsilon_y >^s \\ < 2\varepsilon_{xy} >^s \end{bmatrix}_{\theta=0} - \begin{bmatrix} 1 & 1 & 0 \\ 1 & 1 & 0 \\ 0 & 0 & 0 \end{bmatrix} \\
&\times \begin{bmatrix} < \varepsilon_x >^* \\ < \varepsilon_y >^* \\ < 2\varepsilon_{xy} >^* \end{bmatrix}_{\theta=0} - \begin{bmatrix} 0 & 0 & 0 \\ 0 & 0 & 0 \\ 0 & 0 & 1 \end{bmatrix} \begin{bmatrix} < \varepsilon_x >' \\ < \varepsilon_y >' \\ < 2\varepsilon_{xy} >' \end{bmatrix}_{\theta=0}
\end{aligned} \tag{2-4}$$

4. Off-axis analysis

Eqs. (2-4) represent the governing constitutive equations for the behavior of the on-axis cell. For the off-axis case (see the cell labeled B in Fig. 1), when the cell coordinate system is inclined at an arbitrary angle θ to that of the principal material directions, the procedure of deriving the governing equations is almost identical to that corresponding to the elastic binder case (see part I, Section 4). Hence, we here only list the final result:

$$
\begin{bmatrix} \sigma_x \\ \sigma_y \\ \sigma_{xy} \end{bmatrix}_\theta = \begin{bmatrix} Q_{11}(\theta) & Q_{12}(\theta) & Q_{16}(\theta) \\ Q_{12}(\theta) & Q_{22}(\theta) & Q_{26}(\theta) \\ Q_{16}(\theta) & Q_{26}(\theta) & Q_{66}(\theta) \end{bmatrix} \begin{bmatrix} \varepsilon_x \\ \varepsilon_y \\ 2\varepsilon_{xy} \end{bmatrix}_\theta
$$
$$
- \frac{\sqrt{3}}{12} \begin{bmatrix} 7 - 2S_1 + S_2^2 & 3 - S_2^2 & 2\cos^2(3\theta)S_2 \\ 3 - S_2^2 & 7 + 2S_1 + S_2^2 & 2\sin^2(3\theta)S_2 \\ 2\cos^2(3\theta)S_2 & 2\sin^2(3\theta)S_2 & 3 - S_2^2 \end{bmatrix} \begin{bmatrix} <\varepsilon_x>^n \\ <\varepsilon_y>^n \\ <2\varepsilon_{xy}>^n \end{bmatrix}_\theta
$$
$$
- \frac{\sqrt{3}}{4} \begin{bmatrix} S_1^2 + 0.6S_2^2 & -S_1^2 - 0.6S_2^2 & -0.4S_1S_2 \\ -S_1^2 - 0.6S_2^2 & S_1^2 + 0.6S_2^2 & 0.4S_1S_2 \\ -0.4S_1S_2 & 0.4S_1S_2 & S_2^2 + 0.6S_1^2 \end{bmatrix} \begin{bmatrix} <\varepsilon_x>^s \\ <\varepsilon_y>^s \\ <2\varepsilon_{xy}>^s \end{bmatrix}_\theta
$$
$$
- \begin{bmatrix} 1 & 1 & 0 \\ 1 & 1 & 0 \\ 0 & 0 & 0 \end{bmatrix} \begin{bmatrix} <\varepsilon_x>^* \\ <\varepsilon_y>^* \\ <2\varepsilon_{xy}>^* \end{bmatrix}_\theta - \begin{bmatrix} S_2^2 & -S_2^2 & S_1S_2 \\ -S_2^2 & S_2^2 & -S_1S_2 \\ S_1S_2 & -S_1S_2 & S_1^2 \end{bmatrix} \begin{bmatrix} <\varepsilon_x>' \\ <\varepsilon_y>' \\ <2\varepsilon_{xy}>' \end{bmatrix}_\theta \tag{3-1}
$$

where $Q_{11}(\theta)$, $Q_{12}(\theta)$, $Q_{22}(\theta)$, $Q_{16}(\theta)$, $Q_{26}(\theta)$ and $Q_{66}(\theta)$ are the elements in the off-axis stiffness matrix. Their definition can be found in [1]. The definition for S_1 and S_2 are:

$$
S_1 = \cos^2(3\theta) - \sin^2(3\theta), \quad S_2 = 2\cos(3\theta)\sin(3\theta) \tag{3-2}
$$

The off-axis stiffness matrixes for any given θ are presented in Eq. (3-1). For a packing structure which has a statistically distributed θ represented by a function $f(\theta)$, the averaged stiffness responses then can be evaluated by integrating $f(\theta)$ with both sides of Eq. (3-1) over the range $0 < \theta < \pi/3$. When $f(\theta)$ is constant, e.g. a uniform distribution, the over-all stress and strain relationship can be easily integrated and expressed by:

$$
\begin{bmatrix} \overline{\sigma_x} \\ \overline{\sigma_y} \\ \overline{\sigma_{xy}} \end{bmatrix} = \begin{bmatrix} \overline{Q_{11}} & \overline{Q_{12}} & 0 \\ \overline{Q_{12}} & \overline{Q_{22}} & 0 \\ 0 & 0 & \overline{Q_{66}} \end{bmatrix} \begin{bmatrix} \overline{\varepsilon_x} \\ \overline{\varepsilon_y} \\ \overline{2\varepsilon_{xy}} \end{bmatrix}
$$
$$
- \frac{5\sqrt{3}}{24} \begin{bmatrix} 3 & 1 & 0 \\ 1 & 3 & 0 \\ 0 & 0 & 1 \end{bmatrix} \begin{bmatrix} <\overline{\varepsilon_x}>^n \\ <\overline{\varepsilon_y}>^n \\ <\overline{2\varepsilon_{xy}}>^n \end{bmatrix} - \frac{\sqrt{3}}{5} \begin{bmatrix} 1 & -1 & 0 \\ -1 & 1 & 0 \\ 0 & 0 & 1 \end{bmatrix} \begin{bmatrix} <\overline{\varepsilon_x}>^s \\ <\overline{\varepsilon_y}>^s \\ <\overline{2\varepsilon_{xy}}>^s \end{bmatrix}
$$
$$
- \begin{bmatrix} 1 & 1 & 0 \\ 1 & 1 & 0 \\ 0 & 0 & 0 \end{bmatrix} \begin{bmatrix} <\overline{\varepsilon_x}>^* \\ <\overline{\varepsilon_y}>^* \\ <\overline{2\varepsilon_{xy}}>^* \end{bmatrix} - \frac{1}{2} \begin{bmatrix} 1 & -1 & 0 \\ -1 & 1 & 0 \\ 0 & 0 & 1 \end{bmatrix} \begin{bmatrix} <\overline{\varepsilon_x}>' \\ <\overline{\varepsilon_y}>' \\ <\overline{2\varepsilon_{xy}}>' \end{bmatrix} \tag{3-3}
$$

where ($\bar{\sigma}_x$, $\bar{\sigma}_{xy}$ and $\bar{\sigma}_y$) and ($\bar{\varepsilon}_x$, $\bar{\varepsilon}_{xy}$ and $\bar{\varepsilon}_y$) are the volume averaged stresses and strains, respectively. $\bar{Q}_{11}$, $\bar{Q}_{12}$, $\bar{Q}_{22}$ and $\bar{Q}_{66}$ are the elements in the volume averaged stiffness matrix, and their definition can be found in [1].

It is easily verified that for all the matrixes in Eq. (3-3), the identity remain true: half value of the difference between the first and second diagonal elements is equal to that of the element in first row and second column. This indicates that, for this specific packing distribution $f(\theta)$ = constant, the shear and normal deformations are uncoupled, and the stress–strain relation defined in Eq. (3-3) is isotropic. This indication appears consistent with the theme that the uniform particle distribution (totally random) yields a solid state of being overall isotropic.

5. Model analysis

All the stress–strain equations for the case of on-axis cell, off-axis cell or averaged response are derived so far in form of the integral representation (traditionally, those equations are given in the differentiate format). It is always desirable to see what is the visco-elastic model those integral equations portray. For this purpose, a model study is conducted here. Beginning with Eq. (3-3) and by setting only the variables $\bar{\varepsilon}_x$ and $\bar{\sigma}_x$ non-zero, now, the non-trivial relationship between $\bar{\varepsilon}_x$ and $\bar{\sigma}_x$ reads:

$$\overline{\sigma_x} = \overline{Q_{11}}\overline{\varepsilon_x} - \frac{\sqrt{35}}{8} < \overline{\varepsilon_x} >^n - \frac{\sqrt{3}}{5} < \overline{\varepsilon_x} >^s - < \overline{\varepsilon_x} >^* - 0.5 < \overline{\varepsilon_x} >' \tag{4-1a}$$

The definition for $\overline{Q_{11}}$ can be found in [1] and be expressed as:

$$\overline{Q_{11}} = \frac{5\sqrt{3}}{8}K_n + \frac{\sqrt{3}}{5}K_s + K^* + 0.5Q'_{66} \tag{4-1b}$$

Consolidating Eqs. (4-1a) and (4-1b) yields a matched integral representation between $\bar{\sigma}_x$ and $\bar{\varepsilon}_x$:

$$\begin{aligned}\overline{\sigma_x}(t) = {} & \frac{\sqrt{35}K_n}{8}\left[\overline{\varepsilon_x}(t) - g_n\int_0^t e^{-g_n(t-t_1)}\overline{\varepsilon_x}(t_1)dt_1\right] \\ & + \frac{\sqrt{3}K_s}{5}\left[\overline{\varepsilon_x}(t) - g_s\int_0^t e^{-g_s(t-t_1)}\overline{\varepsilon_x}(t_1)dt_1\right] \\ & + K^*\left[\overline{\varepsilon_x}(t) - g^*\int_0^t e^{-g^*(t-t_1)}\overline{\varepsilon_x}(t_1)dt_1\right] \\ & + 0.5Q'_{66}\left[\overline{\varepsilon_x}(t) - g'\int_0^t \mathrm{e}^{-g'(t-t_1)}\overline{\varepsilon_x}(t_1)dt_1\right]\end{aligned} \tag{4-1c}$$

It is interesting to notice that the four integrals in the right-hand side of Eq. (4-1c) are of the exact representation that characterizes the Maxwell model. Before starting to analyze Eq. (4-1c), let us introduce a model of four Maxwell elements arranged in a parallel connection as shown in Fig. 3, in which K_1, K_2, K_3, and K_4 are the stiffness

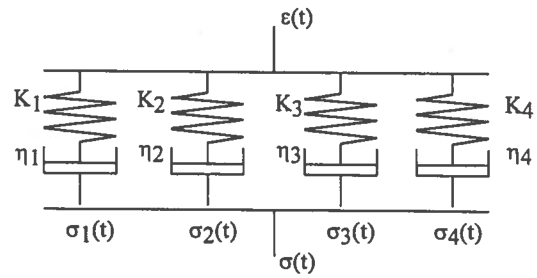

Fig. 3. A visco-elastic system with four Maxwell elements in parallel connection.

constants, and η_1, η_2, η_3, and η_4 are viscous constants respectively. It is easily seen that the following equations are true:

$$\sigma(t) = \sigma_1(t) + \sigma_2(t) + \sigma_3(t) + \sigma_4(t) \tag{4-2}$$

$$\dot{\varepsilon}(t) = \frac{\dot{\sigma}_1(t)}{K_1} + \frac{\sigma_1(t)}{\eta_1} = \frac{\dot{\sigma}_2(t)}{K_2} + \frac{\sigma_2(t)}{\eta_2} = \frac{\dot{\sigma}_3(t)}{K_3} + \frac{\sigma_3(t)}{\eta_3} = \frac{\dot{\sigma}_4(t)}{K_4} + \frac{\sigma_4(t)}{\eta_4} \tag{4-3}$$

where, $\sigma(t)$ and $\varepsilon(t)$ are the model stress and strain. $\sigma_1(t)$, $\sigma_2(t)$, $\sigma_3(t)$ and $\sigma_4(t)$ are the stresses and strains defined in the 1st, 2nd, 3rd and 4th Maxwell elements in Fig. 3, respectively.

Following the manipulations given in Eqs. (1-5)–(1-7), the relation between $\varepsilon(t)$ and $\sigma_1(t)$ given in Eq. (4-3) can be expressed in form of an integral representation with the initial condition $\sigma_1(t=0) = K_1\varepsilon(t=0)$:

$$\sigma_1(t) = K_1\varepsilon(t) - K_1 g_1 \int_0^t \mathrm{e}^{-g_1(t-t_1)}\varepsilon(t_1)dt_1, \quad g_1 = \frac{K_1}{\eta_1} \tag{4-4}$$

Similarly, the relations between $\varepsilon(t)$ and $\sigma_2(t)$, $\varepsilon(t)$ and $\sigma_3(t)$, and $\varepsilon(t)$ and $\sigma_4(t)$ can be arrived:

$$\begin{aligned} \sigma_2(t) &= K_2\varepsilon(t) - K_2 g_2 \textstyle\int_0^t e^{-g_2(t-t_1)}\varepsilon(t_1)dt_1, \quad g_2 = \frac{K_2}{\eta_2} \\ \sigma_3(t) &= K_3\varepsilon(t) - K_3 g_3 \textstyle\int_0^t e^{-g^3(t-t_1)}\varepsilon(t_1)dt_1, \quad g_3 = \frac{K_3}{\eta_3} \\ \sigma_4(t) &= K_4\varepsilon(t) - K_4 g_4 \textstyle\int_0^t \mathrm{e}^{-g_4(t-t_1)}\varepsilon(t_1)dt_1, \quad g_4 = \frac{K_4}{\eta_4} \end{aligned} \tag{4-5}$$

Now, observation to Eqs. (4-2) to (4-5) easily proves that $\varepsilon(t)$ and $\sigma(t)$ are related by:

$$\begin{aligned} \sigma(t) = {} & K_1\varepsilon(t) - K_1 g_1 \int_0^t e^{-g_1(t-t_1)}\varepsilon(t_1)dt_1 + K_2\varepsilon(t) - K_2 g_2 \int_0^t e^{-g_2(t-t_1)}\varepsilon(t_1)dt_1 \\ & + K_3\varepsilon(t) - K_3 g_3 \int_0^t e^{-g_3(t-t_1)}\varepsilon(t_1)dt_1 + K_4\varepsilon(t) - K_4 g_4 \int_0^t \mathrm{e}^{-g_4(t-t_1)}\varepsilon(t_1)dt_1 \end{aligned} \tag{4-6}$$

and the comparison between Eqs. (4-1) and (4-6) readily indicates that the visco-elastic model given in Eq. (4-1) represents a generalized Maxwell models with four Maxwell elements in a parallel connection as described in Fig. 3 with a simple substitution:

$$K_1 = \frac{\sqrt{3}5K_n}{8}, \quad K_2 = \frac{\sqrt{3}K_s}{5}, \quad K_3 = K^*, \quad K_4 = 0.5Q'_{66} \tag{4-7}$$

$$\frac{K_1}{\eta_1} = g_n, \quad \frac{K_2}{\eta_2} = g_s, \quad \frac{K_3}{\eta_3} = g^*, \quad \frac{K_4}{\eta_4} = g' \tag{4-8}$$

The model analysis given from Eqs. (4-1) to (4-8) is done to the pair of $\bar{\varepsilon}_x$ and $\bar{\sigma}_x$. A similar conclusion can also be made to the pair of $(\bar{\varepsilon}_y, \bar{\sigma}_y)$, and $(\bar{\varepsilon}_{xy}, \bar{\sigma}_{xy})$ governed by the second and third equations in Eq. (3-3), respectively. In summary, the overall uni-axial visco-elastic response of the two-phase composite can be graphically depicted as shown in Fig. 3.

6. Asphalt concrete simulation

Asphalt concrete (AC) is a multiphase conglomerate material consisting of mineral aggregates bound together by a petrochemical binder known as asphalt, and is widely used in civil and infrastructure constructions. In this section, the objective is to examine a number of subjects that relate to the modeling of asphalt concrete based on the analyses and results given in this study. The starting point of the asphalt concrete modeling is Eq. (4-1). Asphalt concrete with good quality contains typically 3 to 7% of air void. To incorporate this porosity effect in to consideration, the modification is needed to (4-1c). The last two terms of integral in the right-hand side of Eq. (4-1) represent the non-contact portion of the deformation contribution to its interaction with the stress. However, with the presence of air void in the interstices of aggregate conglomeration, the load transfer mechanism within the system of this conglomeration will mainly take its path through aggregate contacts. As such, these two terms are removed from the stress–strain equation, and correspondingly, the equivalent visco-elastic model corresponding becomes a visco-elastic model of two Maxwell elements in a parallel arrangement as shown in Fig. 4a. By applying the Laplace transform technique to the model given in Fig. 4a, it can be shown that the visco-elastic model in Fig. 4a has an alternative representation which is a four-element model or Burger's model (see Fig. 4b). The relations between the parameters in Fig. 4a and b are derived after quite a few steps of manipulations as follows:

$$K_I = K_1 + K_2, \quad \eta_I = \eta_1 + \eta_2 \tag{5-1}$$

$$\eta_{II} = \frac{g_c(K_1 + K_2)}{(g_1 - g_c)(g_c - g_2)}, \quad g_1 = \frac{K_1}{\eta_1}, \quad g_2 = \frac{K_2}{\eta_2}, \quad g_c = \frac{g_1K_2 + g_2K_1}{K_1 + K_2} \tag{5-2}$$

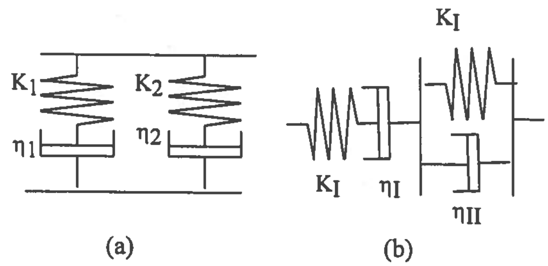

Fig. 4. (a) Two paralleled Maxwell elements; (b) four-element model.

$$K_{II} = \eta_{II} g_c \tag{5-3}$$

Using a four-element model in simulating asphalt concrete has been extensively seen in public literature in the area of asphalt concrete modeling. In fact, it is the most employed approach in analyzing the visco-elastic response of asphalt concrete specimens. However, the basis to use the four-element model has been placed on the empirical justification that this model can fairly capture the overall behavior of asphalt concrete in many aspects, and it is relatively simple. The study presented in this article actually provides a mechanics/physics based justification that rationalizes the applicability of the four-element model in its application in describing asphalt concrete.

Creep tests are often seen in asphalt concrete studies. In his work on creep simulation based on the four-element model, Mamlouk [13] presents the compliance relation as:

$$J(t) = \frac{\varepsilon(t)}{\sigma_0 u(t)} = \frac{1}{K_I} + \frac{t}{\eta_I} + \frac{1}{K_{II}}\left(1 - \exp^{-\frac{t}{\tau}}\right), \quad \tau = \frac{\eta_{II}}{K_{II}} \tag{5-4a, b}$$

where, t is the time variable; τ is retardation time; $J(t)$ is the creep compliance; $\varepsilon(t)$ is the creep strain; $u(t)$ is the step function and σ_0 is the constant stress.

Compared with E_{I} and E_{II}, η_{I} and η_{II} are much more temperature dependant. As such, one important subject in creep analysis is to quantify the dependence of creep compliance on temperature. One well established way to do the quantification is to introduce a set of reference values for η_{I} and η_{II} at a given temperature. η_{I} and η_{II} at other temperatures then can be linearly related to their values at the reference temperature, which mathematically can be expressed by:

$$\eta_{\mathrm{I}} = \eta_{\mathrm{I0}} a_{\mathrm{T1}} \tag{5-5}$$

$$\tau = \tau_0 a_{\mathrm{T2}} \tag{5-6}$$

where, a_{T1} and a_{T2} are called time-temperature shift factors. η_{I0} and τ_0 are the values at the reference temperature, which is typically selected at 21°C. Based on the

argument that asphalt concrete is a thermorheological simple material, Mamlouk further assumes that

$$a_{\mathrm{T1}} = a_{\mathrm{T2}} = a_{\mathrm{T}} \tag{5-7}$$

This assumption is also either explicitly or implicitly granted in most other studies in this subject. Based on Eq. (5-7), a reduced time variable then can be defined:

$$\xi = \frac{t}{a_T} \tag{5-8}$$

and Eq. (5-4) now can be written as:

$$J(t) = \frac{\varepsilon(t)}{\sigma_0 u(t)} = \frac{1}{K_I} + \frac{\xi}{\eta_{I0}} + \frac{1}{K_{II}}\left(1 - \exp^{-\frac{\xi}{\tau_0}}\right), \tag{5-9}$$

The benefit of introducing ξ in the creep compliance is that it establishes a time–temperature correspondence on creep compliance so $J(t)$ determined by the data obtained from the test results done at a given temperature can be used to estimate the creep compliance at a different temperature.

However, we will demonstrate here that the assumption given in Eq. (5-7) is unnecessary, and it is inherently valid without resorting to grant asphalt concrete is a simple thermorheological materials. By observing Eqs. (4-7), (4-8) and (5-1), it is easily seen [also see the definitions given in Eq. (1-6a,b)]:

$$\eta_{\mathrm{I}} = \eta_1 + \eta_2 = \frac{K_1}{g_n} + \frac{K_2}{g_s} = \frac{(C_{nb} + C_{np})\eta_b K_1}{C_{nb} G_b} + \frac{(C_{sb} + C_{sp})\eta_b K_2}{C_{sb} G_b} \tag{5-10}$$

As such, we introduce the shift factor for the asphalt binder only: $\eta_{\mathrm{b}} = \eta_{\mathrm{b0}}\, a_{\mathrm{T}}$ and it will lead to Eq. (5-5):

$$\eta_{\mathrm{I}} = \frac{(C_{nb} + C_{np})\eta_{b0} a_{T1} K_1}{C_{nb} G_b} + \frac{(C_{sb} + C_{sp})\eta_{b0} a_{T1} K_2}{C_{sb} G_b} = \eta_{\mathrm{I0}} a_{\mathrm{T}} \tag{5-11}$$

In an analogy and starting with $\eta_{\mathrm{b}} = \eta_{\mathrm{b0}}\, a_{\mathrm{T}}$, τ can be expressed by:

$$\tau = \frac{\eta_{II}}{K_{II}} = \frac{1}{g_c} = \frac{\eta_b(K_1 + K_2)}{\frac{K_1 C_{nb} G_b}{C_{nb} + C_{np}} + \frac{K_2 C_{sb} G_{nb}}{C_{sb} + C_{np}}} = \frac{\eta_{b0}(K_1 + K_2) a_T}{\frac{K_1 C_{nb} G_b}{C_{nb} + C_{np}} + \frac{K_2 C_{sb} G_{nb}}{C_{sb} + C_{np}}} = \tau_0 a_{\mathrm{T}} \tag{5-12}$$

Therefore, introducing the time shift factor: $\eta_{\mathrm{I}} = \eta_{\mathrm{I0}}\, a_{\mathrm{T}}$ will results in: $\eta_{\mathrm{b}} = \eta_{\mathrm{b0}}\, a_{\mathrm{T}}$, and subsequently: $\tau = \tau_0\, a_{\mathrm{T}}$.

7. Conclusions

The study aims to develop a two-dimensional constitutive theory of two-phase composites with the matrix/binder being Maxwell type of visco-elasticity. The stress–strain relations are established by using the basic cell method, and the effect of Maxwell matrix/binder is incorporated in the stress–strain derivation by using the binder contact laws. It is noticeable that the derivation process is quite lengthy and many integration and matrix manipulations are involved. But, in the end for the case of total randomness in inclusion/particle packing distribution, the final result appears that the composite is isotropic in its homogenization entity. This indicates that introducing Maxwell viscosity in matrix/binder does not change the nature of isotropicity or anisotropicity of the composite. Such an indication is conceivable. In soil/granular mechanics, it has been found that complete uniform distribution of soil/granular packing configuration will lead to the isotropic stress-strain relation defined in a soil/granular pile [14]. It has also been observed that a well mixed asphalt concrete exhibits no favored material orientation directions, which grants the treatment of asphalt concrete as an over-all isotropic medium [15].

Most current treatment on a visco-elastic matrix composite takes an elastic analogy approach that follows the so-called "corresponding theory" [3,4]. In this approach, the integral transform and inverse integral transform are needed, which require lengthy mathematical manipulation that the mathematical complexity may overwhelm the revealing of physics/mechanics for the problem. It appears that the study presents another approach in investigating visco-elastic matrix composites.

The derived stress-strain equations given in this study are in the integral representation, and the benefit is obvious that the visco-elastic effect is concisely expressed in mathematics and well interpreted mechanically. The differentiate format of the stress–strain equations are also available, however, very lengthy that the correspondence to Eq. (3-3) is a set of 8th order of ordinary differentiate equations.

In addition, Eq. (3-3) specifies that there are four components that contribute the visco-elasticity at the composite level, and they can be characterized by: (1) the contact shear viscous time factor (g_s); (2) the contact normal viscous time factor (g_n); (3) the non-contact shear viscous time factor (g'); and (4) the non-contact normal viscous time factor (g^*). One important characteristic of these four time factors is that they can be analytically expressed in terms of the physical and geometrical properties of matrix/binder and particles/inclusions. In fact, this characteristic is useful because it provides a close-form dependence of how an individual parameter of the binder/matrix or inclusions/particles can alter the behavior at the composite level quantitatively [16].

Using the visco-elastic model of multi Maxwell elements in parallel connection to simulate the behavior of asphalt concrete is very popular and can be found in many public literatures [15,16,17]. For example, Bouldin et al. [16] showed that the experimental strain-time data of an asphalt concrete specimen under a Harversine wave load fitted very well with the curve computed by the back analysis based on a model of two Maxwell elements in parallel (Fig. 4a). In the SHRP-A-415, Monismith et al. [15] includes a section of employing three Maxwell elements in parallel to

study the relaxation nature of asphalt concrete. A four-element model, which is equivalent to that of two Maxwell elements in parallel, serves as the basis in predicting the creep compliance in Mamlouk's work [13]. The significance of this study is that this study provides a foundation which justifies the rationality of using the model of multi Maxwell elements to represent asphalt concrete, which is noticed by the fact that the four integrals in Eq. (4-1c) are of the mathematical representation of the Maxwell model.

It has always been an argument on how many Maxwell elements are needed in simulating asphalt concrete. The number for being 2, 3 and 4 is frequently used. From what this study also shows is that the determination of this number really depends on the scope of the simulation on the nature of asphalt concrete. The simplest case is what given in Fig. 4a or b. More importantly, the stiffness and viscosity parameters in the stress–strain relationships at the composite level can be analytically formulated on the basis of physical and geometric properties of the constituents in the composite. Whereby, a parametric study can be pursued to see how the composite responds to the change in value of one single parameter of physical and geometric properties. Such a parametric perturbation can be very useful as an analytic tool [10].

Acknowledgements

A portion of the funding for conducting this study is from the Air Force Office of Scientific Research, under Wright Laboratory Task 2302CW.

References

[1] Zhu H, Rish JW III, Dass WC. Constitutive relation for two-phase particular materials. I: elastic binder. Computers and Geotechnics 1997;20(3):303–23.
[2] Zhu H, Chang SC, Rish JW III. Normal and tangential compliance for conformation binder contact: elastic and visco-elastic binder. Int J Sol Struct 1996;33:4351–63.
[3] Schapery RA. Viscoelastic behavior and analysis of composite materials. In: Sendeckyj GP, editor. Mechanics of composite materials. New York: Academic Press, 1974.
[4] Hashin Z. Analysis of composites materials — a survey. J Appl Mech 1983;50:481–98.
[5] Murayama S. Formulation of stress–strain–time behavior of soils under deviatoric stress condition. Soils and Foundations 1983;23:43–53.
[6] Kuhn MR. Micromechanical Aspects of Soil Creep. PhD thesis, University of Californian at Berkeley, 1987.
[7] Meegoda NJ, Chang KG. Simulation of the behavior of asphalt concrete using discrete element methods. Proceedings of the Second International Conference on Discrete Element Methods, Mit, Boston, MA, 1993.
[8] Lacerda WA. Stress-relaxation and Creep Effects on Soil Deformation. PhD thesis, University of Californian at Berkeley, 1978.
[9] Murayama S, Michihiro K, Sakagami T. Creep characteristics of sands. Soils and Foundations 1984;24:1–13.
[10] Zhu H, Nodes JE. Contact based analysis of asphalt pavement with the effect of aggregate angularity. Mechanics of Materials 2000;32(3):193–202.

[11] Little DN, Prapnnachari S, Letton A, Kim YR. Investigation of the Microstructural Mechanisms of Relaxation and Fracture Healing in Asphalt. AFOSR-89-0520, 1993.
[12] Anderton GL. Alternate/Modified Binders for Asphalt Airfield Pavements, ESL-TR-89-40, 1990.
[13] Mamlouk MS. Rheology of cold-recycled pavement materials using creep test. Journal of Testing and Evaluation 1984;12(6):341–7.
[14] Chang CS, Misra A. Application of uniform strain theory to heterogenous granular solids. J Engng Mech ASCE 1990;116:2310–7.
[15] Monismith CL, et al. Permanent Deformation Response of Asphalt Aggregate Mixes. SHRP-A-415, Strategic Highway Research Program, NRC, Washington, 1994.
[16] Bouldin MG, Rowe GM, Sousa JB, Sharrock MJ. Mix rheology-a tool for predicting the high temperature performance of hot mix asphalt. AAAP 1993;63:182–223.
[17] Hopman PC, Pronk AC, Kunst PAJC, Molenaar AAA, Molenarr JMM. Application of the Viscoelastic Properties of Asphalt Concrete. 77th Int. Conference on Asphalt Pavements, 1992, 73-89.